RSC Advances

ROYAL SOCIETY OF CHEMISTRY

www.rsc.org/advances

Journal Name

ARTICLE

On stereocomplexed polylactide materials as support for PAMAM dendrimers: synthesis and properties

Received 00th January 20xx,
Accepted 00th January 20xx

DOI: 10.1039/x0xx00000x

www.rsc.org/

Lorenza Gardella,[a] Andrea Basso,[a] Mirko Prato[b] and O. Monticelli[a*]

Stereocomplexed polylactide materials functionalized with poly(amido-amine) (PAMAM) dendrimer units were prepared by solution blending dendritic poly(D-lactide) (PDLA) star oligomers into a commercial poly(L-lactide) (PLLA), where the dendritic PDLA star oligomers were built up by ring-opening polymerization of D-lactide using a PAMAM dendrimer as macroinitiator. Whereas the synthesized poly(D-lactide)s (whose star-like architecture, comprising the PAMAM dendrimer as the core and a multi-arm PDLA shell, was demonstrated by means of ^{1}H NMR spectroscopy) were observed to structure/crystallize hardly, their blended films, as revealed by DSC and WAXD measurements, proved capable of easy stereocomplexation in solution and melt crystallization alike. The stereocomplex, whose content and characteristics are greatly affected by the structure of the PDLA stars, affords improved thermal and chemical resistance, while simultaneously providing a strong link for the PAMAM units to the polymer matrix. The PAMAM dendrimers can thus show themselves up, while being anchorated onto a water/(solvent) insoluble, easy-processable polymeric support, which, in addition, is bio-based and bio-degradable and keeps the characteristics of biocompatibility. Indeed, thanks to the presence of the PAMAM functionalities, and unlike the neat polylactide, the resulting materials were shown to possess significant water-absorbency and Pd(II)-uptake-ability. This latter property was exploited for the removal of Pd catalyst from a homogeneous reaction system.

Introduction

Poly(amido-amine) (PAMAM) dendrimers are a family of dendrimers (that is, synthetic macromolecules consisting of a highly and perfectly branched tree-like structure, with a large number of external functional groups and controllable internal cavities), built up by polyamide branches with tertiary amines as focal points.[1,2] They are very popular (especially in biology and medicine) because of their being commercially available, water-soluble, non-toxic/non-immunogenic, and able to bind/host a wide variety of guest molecules (*e.g.*, biologic substrates, drugs, metals, *etc.*).[2-4] In particular, the exceptional capability of the PAMAM dendrimers to coordinate metal ions (*e.g.*, Cu^{2+}, Pd^{2+} and Pt^{2+}) has attracted a great deal of interest because of its wide applicative potential (for example in the synthesis of metal nanoparticles).[4,5] Among those, the sorption of palladium – Pd^{2+} forming strong interactions with the amino groups of the dendrimer, such that the resulting complex is stable under both reducing and oxidizing conditions and no leaching of Pd ions is detectable – stands out, due to the fundamental role palladium plays in catalysis.[5-7] However, the high solubility, not only in water but in a variety of common organic solvents, as an intrinsic property of the dendrimers resulting from their characteristic globular conformation, makes their recovery from solutions difficult, it requiring time-consuming and/or expensive techniques such as selective precipitation, dialysis and membrane nanofiltration, whose yield is furthermore often unsatisfactory.[4,8] Immobilization of the dendrimers on insoluble solids (most typically silica particles) offers an easy and practical solution to overcome this limitation,[8] thus further opening their applications, not only (following the reduction of the bound metal ion) as recyclable heterogeneous catalysts,[9-11] but also to the most recently addressed use as easy-separable chelating systems, for example for the purification of water from heavy metal ions,[12,13] or metal ion separation/concentration for purposes of analysis,[14] as well as catalyst separation from the reaction media – this latter being the issue we specifically tackled in our work. In fact, widespread (commercial/industrial) use of highly active and selective transition-metal-based homogeneous catalysts is still restrained by the complex and costly problem of their removal from the reaction mixture, which problem arises from both the obvious need to avoid contamination of the reaction products, and from the need to recycle them so as to increase their productivity and economical attractiveness.[8]

PAMAM dendrimers (either hydroxyl- or amino-terminated) have been used as multifunctional macroinitiators in the ring-opening polymerization of lactide, whereby multi-arm dendritic star-like polylactide (PLA) polymers were prepared, made up of a large

[a]*Dipartimento di Chimica e Chimica Industriale, Università di Genova, Via Dodecaneso, 31, 16146 Genova, Italy*
[b]*Nanochemistry Department, Istituto Italiano di Tecnologia, Via Morego, 30, 16163 Genova, Italy*

Electronic Supplementary Information (ESI) available: [Structure of generation 2 PAMAM dendrimer. ^{1}H NMR spectra of the multi-arm star-like poly(D-lactide)s. Optical micrograph of the multi-arm star-like poly(D-lactide)s. TGA curves of the equimolar PAMAM-D/PLLA blend films. Table reporting the results of the water absorption test. See DOI: 10.1039/x0xx00000x

number of arms ("multi-arm") grown on the dendritic core ("dendritic").[15-18] Star polymers are a class of (regular) branched polymers in which the branches (arms – having essentially identical lengths) radiate from a central core, having chemico-physical properties completely different from linear analogues.[2] Indeed, due to their peculiar structure, with still relatively short chains however high the mass, more compact shape and increased concentration of functional end-groups, star polymers feature enhanced solubility, lower viscosity – chain entanglement being hardly operative – lower crystallizability and thermal/hydrolytic stability, which features make them highly attractive in the fields of self-assembly and drug-delivery, but, in their neat form, totally unsuitable for use as structural materials.[2,19] Thus, because of their amphiphilic core-shell structure, the dendritic star-like PLAs, have been mainly addressed as potential systems for encapsulation/controlled release of guest molecules.[17,20,21]

Branched PLA structures behaving as plasticizers,[22,23] poly(L-lactide) (PLLA) stars have been also proposed as (miscible) additives for linear PLLA, with a dual action as plasticizers and simultaneously nucleating agents.[24,25] More interesting, stereocomplexation was shown to occur when branched/star-like PLA (PLLA or PDLA – poly(D-lactide))] polymers are introduced into their linear enantiomeric counterpart.[23,26,27,28] The appeal of the stereocomplex-type PLA, formed upon mixing the two (PLLA and PDLA) enantiomers, resides in its superior properties/performances with respect to the two single polymers: the stereocomplex form has a melting temperature of about 230 °C (that is, 50 °C higher than that of PLLA and PDLA homo-crystals), higher stability/lower solubility in good solvents for either mere PLLA or PDLA, as well as enhanced crystallization rate, mechanical properties and the resistance to hydrolysis.[29] Moreover, in the case of blends of PLLA with 4- and 6-arm PDLA star "oligomers", the melting temperature of the obtained stereocomplexes was found to depend on the arm length of the stars, similar as their melting enthalpy (*i.e.*, content; strongly affected also by the blending ratio and number of arms – lower for 6-arm stars than for 4-arm ones), such that the resulting hydrolytic behavior could be customized through the architecture of the PDLA partners.[27,28] Grafting PDLA chains from active surface groups of various nanofillers, to be subsequently incorporated into commercial PLLA, proved an excellent method to obtain a good particle dispersion and simultaneously, thanks to the stereocomplex formation, a strong filler/matrix interaction, both of which are essential requirements to achieve an effective improvement of properties. PLA-based nanocomposites with (multi-walled) carbon nanotubes,[30,31,32] graphene oxide[33] and [POSS-core/poly(ε-caprolactone-co-lactide)-shell] rubber-like nanoparticles[34] were thence prepared, combining in a synergic way the superior thermal and mechanical properties of the stereocomplex-PLA with either the reinforcing and nucleating effect of the first two fillers or the toughening action of the latter.

With this in mind, and aiming to address the problem of dendrimer supporting, we grew PDLA arms onto a generation 2 PAMAM dendrimer, and then introduced the resulting multi-arm star-like poly(D-lactide)s into a commercial, linear PLLA by solution blending, expecting this approach to enable us to "transfer" into a self-supporting, stereocomplex PLA material, together with the property-to-architecture versatility afforded by the star-like systems, the properties specific of the PAMAM dendrimers (e.g. metal-ion-binding-capability). The PAMAM dendrimers could thus perform their functions, while being anchorated onto a water/(solvent) insoluble, easy-processable (for example into film/fiber form; as compared to traditional supports such as silica) polymeric support, which, in addition, is bio-based and bio-degradable and keeps the characteristics of biocompatibility.[35] These materials were characterized by a number of techniques and tested as easy-recoverable films for the removal of Pd catalyst from a homogeneous reaction system.

Experimental

Materials.

D-lactide (D-la) (purity >98%) was kindly supplied by Purac Biochem (The Netherlands). Before polymerization, the monomer was purified by three successive recrystallizations from 100% (w/v) solution in anhydrous toluene and dried under vacuum at room temperature. Second generation PAMAM dendrimer containing 16 amidoethanol surface groups (here simply referred to as PAMAM-OH or PAMAM; structure reported in Figure 1S), commercialized from Sigma-Aldrich as a 20 wt.% solution in methanol, was evaporated under vacuum at 50 °C for 24 h prior to use, to remove the solvent completely. Tin(II) 2-ethylhexanoate ($Sn(Oct)_2$) (95%; from Sigma-Aldrich) was used without further treatments. Poly(L-lactide) and poly(D-lactide), both with average molecular weight of $1{\cdot}10^5$ g/mol (L_{100K} and D_{100K}, respectively), were obtained from Purac (Synterra PLLA 1010 and Synterra PDLA 1010) in pellet form. All the solvents (*i.e.*, anhydrous toluene (≥99.7%), chloroform, methanol, hexane, dichloromethane and acetonitrile) were purchased from Sigma-Aldrich and used as received. Palladium(II) acetate ($Pd(OAc)_2$) (98%) is also a product from Sigma-Aldrich, to be used as it is.

Synthesis of dendritic star-like poly(D-lactide)s.

Star-like poly(D-lactide) was synthesized by ring-opening polymerization (ROP) of D-lactide, using the hydroxyl-terminated PAMAM dendrimer as macroinitiator and $Sn(Oct)_2$ as a catalyst, in bulk at 130 °C – where 130 °C was found to be the optimal reaction temperature for the ROP of enantiopure lactide with dendritic initiators and $Sn(Oct)_2$ catalyst.[15,21] Two different star co-products were then obtained by fractionation of the polymerization output.

In detail, about 2.5 g of D-la (previously recrystallized and dried) were charged under argon flow into the reactor (*i.e.*, a 50-ml two-neck round-bottomed flask equipped with a magnetic stirrer) containing a predetermined amount of accurately weighed and in-situ dried PAMAM-OH. The feeding ratio of the D-la monomer to the PAMAM-OH initiator was adjusted to 200 to 1. After the introduction of D-la, the flask was evacuated for 15 minutes and purged with argon, and the exhausting/refilling process repeated three times in order to completely remove traces of water from the reaction environment. The reaction vessel was then immersed into a thermostatically controlled oil bath set at 130 °C, under vigorous stirring: as soon as the mixture was completely molten and homogenized, about 0.2 ml of a freshly prepared solution of $Sn(Oct)_2$ in toluene ($[D\text{-la}]/[Sn(Oct)_2] = 10^2$) were added under argon

through a micro-pipette, and the reaction allowed to proceed for 24 hour under inert atmosphere, before cooling it down.

First, the crude product was dissolved in chloroform and poured into an excess of cold methanol: after filtering and drying in vacuum at 40 °C to constant weight, the as-purified polymer (designated as PAMAM-D1) was obtained as a white fine powder with a gravimetric yield of ~20%. Thereafter, the filtrate was evaporated under vacuum until complete removal of the methanol, and the recovered product further dissolved in chloroform and reprecipitated into hexane, to be finally filtered, repeatedly washed with cold methanol and dried: a yellowish and sticky polymer was obtained (designated as PAMAM-D2), whose gravimetric yield was estimated to be ~40%.

Preparation of PAMAM-D/L_{100K} blend films.

A series of PLLA films with different amounts of the two dendritic star-like poly(D-lactide)s was prepared by solution casting. The PAMAM-D sample and commercial L_{100K} (0.2 g overall) were dissolved in dichloromethane (10 ml), cast onto a glass Petri dish, and allowed to dry in air. Then, the solidified films were further dried in vacuum for 4 hours at 40 °C and 4 hours at 80 °C, to completely remove the solvent. Films having thickness of about 100 μm were fabricated. PAMAM-D/PLLA blends containing 5, 25 and 50 wt% of PAMAM-D1 (labelled as D1_5, D1_25 and D1_50, respectively) and 5 and 50 wt% of PAMAM-D2 (labelled as D2_5 and D2_50) were prepared.

For comparison, films were also produced, following the same procedure as above, of neat L_{100K} or blending L_{100K} and D_{100K} at 50 wt% (L_{100K} /D_{100K}).

Pd(II) uptake test.

To test their capacity to uptake Pd(II), two strips of the L_{100K}, L_{100K}/D_{100K} D1_50 and D2_50 films (previously dried overnight), having area of 1.5 × 0.375 cm^2, were immersed into 10 ml of an acetonitrile solution containing 10 mg of Pd(II) acetate, in order to simulate a typical homogeneously-Pd-catalyzed organic reaction, either at room temperature for 48 hours, or for 1 hour by heating at reflux (that is, at 80 °C). After this time, the specimens were recovered from the solution, washed twice by soaking into clean acetonitrile for 48 hours, and vacuum-dried overnight at 40 °C. The (dry) sample weights were determined both before and after the immersion and washings.

Measurements.

FTIR spectra were recorded on a Bruker IFS66 spectrometer in the spectral range 400-4000 cm^{-1}.

^{1}H NMR spectra were collected with a Varian NMR Mercury Plus instrument, at a frequency of 300 MHz, in $CDCl_3$ solutions containing tetramethylsilane as internal standard.

Thermal gravimetrical analysis (TGA) was performed with a Mettler-Toledo TGA 1 thermogravimetric analyzer, under a flow of nitrogen of 80 ml/min. The weight loss of the samples (having initial masses of ca. 10 mg) was measured in isothermal mode at a holding temperature of 200 °C.

Differential scanning calorimetry (DSC) measurements were performed with a Mettler-Toledo TC10A calorimeter calibrated with high purity indium and operating under flow of nitrogen. The sample weight was about 5 mg and a scanning rate of 10 °C/min was employed in all the runs. The samples were heated from 25 °C to a temperature at which the melt was allowed to relax for 1 minute (that is, 180 °C for the PAMAM-D samples and 250 °C for the film samples), then cooled down to -10 °C, and finally heated up again to 180/250 °C (second heating scan). The reported Tg (glass transition temperature), and Tm (melting temperature) values were defined as the midpoints of the sigmoidal curve and maxima of the endotherms, respectively. When indicated, the degree of crystallinity was calculated by using ideal enthalpies of fusion of 93 J/g for homo-crystals and 142 J/g for stereocomplex crystals.[29] For all samples, the degree of crystallinity was normalized to the PLA content (in g/g).

Morphological observations were done by means of polarized optical microscopy, employing a Polyvar Pol microscope equipped with a Mettler Toledo hot-stage (FP 82). The samples were sandwiched to about 50 μm in thickness between two microscope glasses, annealed for 1 minute in the melt (180 °C for the PAMAM-D samples and 230 °C for the films), and then cooled at 20 °C/min to the isothermal crystallization temperature (with the lower-limit of the explored temperature range being generally fixed by the appearance of crystallization during cooling), at which morphological developments were monitored and recorded through a computer-controlled digital camera (Motic) taking micrographs at chosen time intervals.

Wide-angle X-ray diffraction (WAXD) measurements were performed in reflection mode using a Philips PW 1830 powder diffractometer equipped with a nickel-filtered Cu-Kα source (λ = 0.1542 nm) in a 2θ angle range of 5-30°. The crystalline phase content was calculated after deconvolution of the WAXD patterns (using the software package Peak-Fit) as the ratio between the areas of the crystalline peaks to the total area under the curve.

The water absorption was measured by immersing film specimens having area of 1.5 × 1.5 cm^2 in distilled water at room temperature for 48 h, and expressed as increase in weight percent according to the formula:[36]

$$Water \text{ adsorption } (\%) = [(W_{WET} - W_{dry0})/W_{dry0}] \times 100 \quad (1)$$

where W_{wet} is the wet weight measured (immediately – to avoid evaporative losses) after withdrawing the films from water and gently wiping off the surface water with a tissue, and W_{dry0} is the initial weight of the specimens, measured after vacuum-drying the films for 24 h at 40 °C. In order to evaluate the eventual presence of water-soluble components in the samples, after the immersion the films were further dried (for another 24 h at 40 °C in vacuum), and the percentage of mass lost calculated as:[36]

$$Weight \text{ loss } (\%) = [(W_{dry0} - W_{dry})/W_{dry0}] \times 100 \quad (2)$$

where W_{dry} is the dry weight of the specimens as measured after the second drying treatment. For those samples whose dry weight after the immersion was lower than the initial one, the water-absorption value was calculated as the sum of the increase in weight on immersion plus the weight of the lost matter,[36] though, obviously, this procedure does not allow quantifying the water that could have been absorbed by the soluble part. The values

presented are the average over the measurements on four films for each sample.

Elemental analysis of the samples tested for Pd(II) uptake was carried out via Inductively Coupled Plasma Optical Emission Spectrometry (ICP-OES), performed with a iCAP 6300 DUO spectrometer (Thermo Fisher). The film specimens (about 5 mg in weight) were dissolved in 0.5 ml of a concentrated HCl/HNO3 3:1 (v/v) (Carlo Erba superpure grade) mixture and left to stand overnight at room temperature, in order to completely disrupt any organic component. Afterwards, (4.5 mL) MilliQ grade water (18.3 M Ohm) was added, and the solution filtered using a 0.45-µm-pore-size filter. Palladium concentration was measured using the most sensitive Palladium emission line (*i.e.*, 340.4 nm).

Results and discussion

In this work, stereocomplexed PLA materials, consisting of high molecular weight PLLA and dendritic PDLA star oligomers, were prepared. At first, two different poly(D-lactide)s were synthesized via ROP of D-lactide starting from an hydroxyl-terminated PAMAM dendrimer, followed by fractionation. Then, the resulting products, whose star-like architecture comprises the PAMAM dendrimer as the core and an exterior shell formed by numerous PDLA arms, were introduced into a commercial PLLA through solution blending, to obtain PLA-based films affording the thermal and chemical resistance of the stereocomplex together with the properties specifically imparted by the PAMAM dendrimers.

Synthesis and characterization of dendritic star-like poly(D-lactide)s.

The $Sn(Oct)_2$-catalyzed ROP of D-la employing the flexible generation 2 PAMAM-OH (fitted with 16 terminal hydroxyl groups) as the macroinitiator was carried out as described in the Experimental Section. According to the FTIR spectrum of the crude reaction product (not shown) – with the absorption band at 935 cm^{-1}, characteristic of the monomer but absent in the polymer,[37] having negligible magnitude – the conversion of D-la was close to completion. Next, the polymerization product was subjected to fractionation upon precipitation into methanol,[38] whereby PAMAM-D1 separated as a solid, whereas part of the polymer (PAMAM-D2; which part was expected to consist of the lower molecular weight component) remained in solution – the star topology and the presence of PAMAM in the framework accounting for methanol-solubility – to be then recovered by solvent removal and undergo a purification treatment too. Indeed, the obtainment of two different products may be related to the presence of two different "kinetic populations", resulting from a possible incomplete/uneven initiation, differing for the number of initiating hydroxyl groups and propagating with different rates.[39]

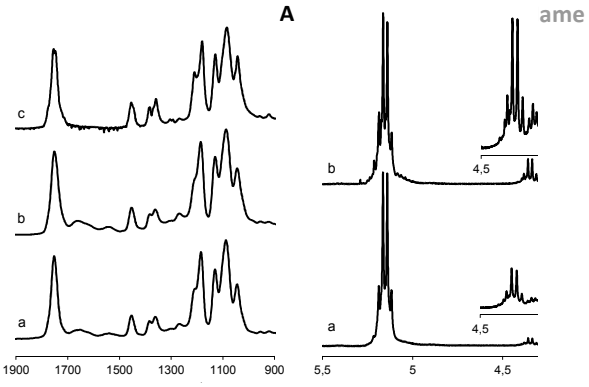

Fig. 1. FTIR spectra of samples PAMAM-D1 (a), PAMAM-D2 (b) and commercial L_{100K} (c) in the spectral region 1900-900 cm^{-1} (A); ^1H NMR spectra (region at δ 5.5-4.0 ppm) of samples PAMAM-D1 (a) and PAMAM-D2 (b) with enlargement insets (at δ 4.5-4.0 ppm) (B).

Figure 1A shows FTIR spectra of the two co-products PAMAM-D1 (a) and PAMAM-D2 (b), together with that of commercial L_{100K} (c): besides the intense absorption band for the stretching of the ester carbonyl at 1757 cm^{-1}, which is a common feature to all the three spectra, two additional peaks of lower intensity can be observed at 1650 and 1538 cm^{-1} in traces a and b (corresponding to amide carbonyl stretching and amide N-H bending, respectively),[40] to be related to the poly-(amidoamine) structure of the PAMAM molecule. As the two PAMAM-D samples have been purified with methanol, so as to remove eventual residues of unreacted D-la and PAMAM-OH, FTIR spectroscopy seems substantiating the covalent incorporation of PAMAM into the polymerized PDLA frameworks. Moreover, it is possible to note that the relative intensity of the two peaks from the PAMAM moiety, with respect to the ester carbonyl band from the polylactide chain (normalized to 1 in all spectra), is slightly higher in the spectrum of PAMAM-D2 (b) compared to that of PAMAM-D1 (a), which supports the higher content of PAMAM in PAMAM-D2, thence its lower molecular weight.

The two PAMAM-D samples were characterized by means of ^1H NMR spectroscopy and the signals identified according to the literature.[15,16,41] In addition to the peaks characteristics of PLA (at δ 1.50-1.58 ppm, 4.35 ppm and 5.16 ppm – assigned as methyl protons, methine protons at the chain ends and methine protons in the chain, respectively), several new signals could be detected, ascribable to the presence of the PAMAM structural unit (even though a complete assignment was not possible due to the poor solubility of PAMAM in chloroform, causing its peaks to be broad and not obviously distinguished).[15,17] The integral ratio of these signals to those from PDLA was higher in the case of PAMAM-D2, as expected for lower molecular weights. The two ^1H NMR spectra (region at δ 5.5-4.0 ppm) are presented in Figure 1B (complete spectra given in Figure 2S). Together with the resonances for the chain and terminal methine protons of PDLA, both spectra display a multiplet at about 4.24 ppm, attributed to the terminal methylene protons of PAMAM-OH (whose signal appears at about 3.56 ppm when adjacent to hydroxyls) shifted upon formation of ester linkages. This evidence definitively allows assessing the successful preparation of star-like poly(D-lactide)s, with the ROP of D-la effectively induced from the hydroxyl tails of the PAMAM-OH initiator. However, it must be pointed out that not all the possible hydroxyl initiation sites took part in the polymerization (as generally

reported for the synthesis of multi-arm PLA stars, due to steric hindrance),[15,16,21] which could be inferred from the observation that the PAMAM-OH terminal methylene proton signal at about 3.56 ppm was not completely disappeared. Unfortunately, the poor resolution of the peaks in the region at δ 4.0-2.0 ppm prevented the calculation of the ratio of reacted to unreacted hydroxyl groups, and the average number of arms of the PAMAM-D samples needed to be derived by combining the information from ^{1}H NMR and TGA as explained in the following. The mean degree of polymerization (DP) of the PDLA arms, based on ^{1}H NMR spectroscopy, was calculated by comparison of the peak integral of the methine protons in the polylactide chain with those at the chain end (at δ 5.16 and δ 4.35 ppm, respectively): the number average molecular weight (Mn) of PAMAM-D1 and PAMAM-D2 (per arm) was estimated to be about 2500 and 1000 g/mol, respectively (values reported in Table 1, where the little uncertainty is due to the partial overlap between the resonance of the terminal methine protons of PDLA and that of the terminal methylene protons of PAMAM-OH) – the arms of PAMAM-D2 being much shorter, going along with the fractionation process.

Thermal gravimetric analysis was exploited to determine the content of PAMAM in the polymers. Indeed, since the two structural parts (the polyester branches and the PAMAM core) have very different thermal stabilities (with the PAMAM moiety being more thermally resistant), by isothermal holding at 200 °C it is possible to degrade selectively only the PDLA component. Figure 2B shows the TGA curves of the two PAMAM-D samples during the isothermal measurement: the mass loss corresponds to the degradation of the PDLA arms, while the remaining weight (dotted lines drawn to guide the eyes) belongs to the PAMAM units (as identified by FTIR spectroscopy – results not shown), thus allowing quantifying their mass percentage in the samples. As shown in Table 1, a PAMAM content of about 11 and 16% was found in PAMAM-D1 and PAMAM-D2, respectively.

From these values, the overall Mn of the two PAMAM-D samples was obtained (see Table 1), and, on the basis of the arm length calculated from ^{1}H NMR spectroscopy, it was estimated that PAMAM-D1 and PAMAM-D2 are characterized by an average number of polylactide arms (n) attached to the surface of PAMAM-OH of about 11-12 and 14-15 arms, respectively (which values are in agreement with those reported by Zhao et al. for star-like PLLAs started from the same generation 2 PAMAM-OH).[16] This result confirms what found above, that not all the total (16) hydroxyl sites carry PDLA branches – the higher the number of initiating hydroxyls the shorter the resulting arms (which can be intuitively figured out by taking into account the dependence of the polymerization kinetics on the steric hindrance,[42] where the more densely packed the growing chains are on the surface of PAMAM-OH, the slower their polymerization rate is expected to be).

The molecular characteristics of PAMAM-D1 and PAMAM-D2 are listed in Table 1. By means of ROP of D-la with PAMAM-OH and subsequent fractionation in methanol (whereas the molecular weight of dendritic star-like PLAs was generally regulated by variation of the monomer-to-initiator-molar ratio and/or the generation of the dendrimer initiator),[15,17,21] two multi-arm star "oligomers" with a molecular weight of about 30.000 and 20.000 g/mol, incorporating the PAMAM moiety as the core and differing for the length and number of the attached PDLA arms, were targeted. As it has been shown that from twelve arms on PLA stars take on a more globular conformation,[43] it can be easily anticipated that the regular packing/structuring of these materials will be challenging.

Table 1. Molecular characteristics of the synthesized dendritic star-like poly(D-lactide)s.

Sample	$DP_{NMR(arm)}$ [a]	$Mn_{NMR(arm)}$ [b] [kg/mol^{-1}]	wt% $PAMAM_{TGA}$ [c]	Mn_{TGA} [d] [kg/mol^{-1}]	n [e]
PAMAM-D1	15-18	2.19-2.55	10.8	30.30	11-12
PAMAM-D2	7-8	1.07-1.20	16.3	19.98	14-15

[a] Average degree of polymerization of D-la (per arm) evaluated from ^{1}H NMR spectroscopy [by comparing the peak integral of the methine protons in the chain (at δ 5.16 ppm) with that of the methine protons at the chain end (at δ 4.35 ppm)]. [b] Numeric average molecular weight of each PDLA arm calculated as: $Mn_{NMR(arm)} = DP_{NMR(arm)} * 144.13$, where 144.13 is the MW of D-la. [c] Measured by TGA analysis. [d] Numeric average molecular weight of the PAMAM-D sample calculated as: Mn_{TGA}= (3271.93 * 100)/ wt% $PAMAM_{TGA}$, where 3721.93 is the MW of PAMAM-OH. [e] Average number of PDLA arms calculated as: $n = (Mn_{TGA} - 3271.93)/ DP_{NMR(arm)}$, where 3721.93 is the MW of PAMAM-OH.

The thermal properties of the synthesized multi-arm star-like poly(D-lactide)s have been characterized by means of DSC and TGA. Figure 2A shows the DSC thermograms during both the first and the second heating scans (that is, on heating the as-prepared samples, and following cooling from the relaxed melt to -10 °C), whereas the values for the characteristic thermal transitions are provided in Table 2. Both samples display melting endotherms during the first heating scan, indicating the presence of some crystalline order, which (as in the literature it has been demonstrated that the structure of PLLA crystals is independent of arms)[16,44,45] can be assigned as the most common crystalline α-form of enantiopure PLLA/PDLA.[46] The relatively low melting temperatures observed (spanning the range 40-120 °C and 100-140 °C for PAMAM-D2 and PAMAM-D1, respectively) need to be imputed to the low molecular weight of the PDLA arms and to the branched structure of the PAMAM-D samples, both of which factors negatively affect crystal thickness and perfection.[15,16,42,47,48] Going along with the shorter chain length of its arms and with its higher density of branching points and terminal groups, the sample PAMAM-D2 exhibits lower melting point than PAMAM-D1 (whose Tm is at about 130 °C, in good agreement with the sample reported by Zhao et al.,[16] having similar molecular characteristics), as well as a much broader signal and lower enthalpy of fusion (see Table 2).

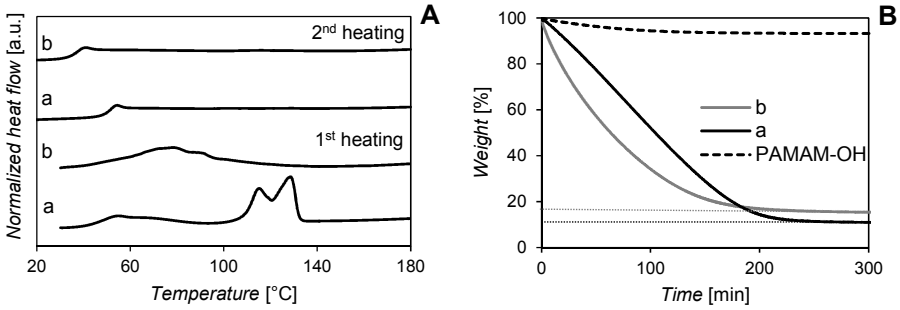

Fig. 2. DSC thermograms of PAMAM-D1 (a) and PAMAM-D2 (b) both as-prepared (first heating scan) and after melt-cooling (second heating scan) (A; the heat flow is normalized to the PDLA content), and their TGA curves recorded on isothermal holding at 200 °C (B). For comparison, also the TGA curve of PAMAM-OH is reported (dashed line).

Table 2. Thermal properties of the PAMAM-D samples and their blend films with L_{100K}.

	1st heating[a]			2nd heating[b]				
Sample	T_g [°C]	T_m[c] [°C]	ΔH_m[c,d] [J/g]	T_g [°C]	T_{cc}[c] [°C]	ΔH_{cc}[c,d] [J/g]	T_{Hm}[c] [°C]	ΔH_m[c,d] [J/g]
L_{100K}	n.d.[e]	177.8	48	61	104.4	28	176.6	50
L_{100K}/D_{100K}	n.d.[e]	174.9/224.0	4/58	61	102.8	24	175.5/221.1	38/20
PAMAM-D1	47	128.7	42	51	-	-	-	-
D1_5	n.d.[e]	177.1/192.0	42/3	57	101.6	32	172.1/185.9	45/1
D1_25	n.d.[e]	179.9/197.7	17/28	51	94.3/104.1	14/12	161.4/182.6	20/18
D1_50	n.d.[e]	200.6	54	47	88.3	30	186.5	37
PAMAM-D2	n.d.[e]	78.7	38	37	-	-	-	-
D2_5	n.d.[e]	176.4	40	57	101,8	28	171.8	45
D2_50	n.d.[e]	171.8	36	43	101.6	16	148.1/161.0	14/6

[a] First heating scan (from 25 °C to 180/250 °C) of the as-prepared PAMAM-D samples and solution-cast films. [b] Heating (from -10 °C to 180/250 °C) of the melt-cooled samples. [c] The subscripts m and cc indicate the values measured during melting and cold-crystallization, respectively; for the blend films, when two values are reported, they signify the presence of two discernable peaks, a lower-temperature (first value) and higher-temperature (second value) one. [d] ΔH is the enthalpy, normalized to the PLA content. [e] Not determined.

Conversely, only a glass transition can be detected in the second heating run of the two samples, whereas there is no sign of cold crystallization/melting phenomena, which observation suggests that, in spite of the relatively low overall molecular weight of the samples, their crystallization rate is too low for any crystallinity to develop on cooling from the melt and subsequent heating from the glassy state alike. Indeed, the much decreased crystallizability, on increasing the number of arms, of PLLAs having star-like topology (compared to their linear counterparts) is well-documented[42,47,48] – the ordering process being slowed down by the reduced mobility of the chains when tethered together to the central core, and by the need to exclude the branching points and end groups (namely defects) from crystalline regions – till complete suppression of crystallization in multi-arm dendritic samples.[15-17,21,45,49] As the two samples are fully amorphous (then totally free from the constraints imposed by crystalline domains), their glass transition values must reflect uniquely the contribution from the free volume of the system, thence the lower Tg of PAMAM-D2 (see Table 2).

As determined by TGA, the sample PAMAM-D2 is less thermally stable than PAMAM-D1 (see Figure 2B: the decomposition stage of PAMAM-D1 is entirely shifted towards longer times), in agreement with the role played by hydroxyl terminal groups in thermal degradation.[50]

The morphology of the PAMAM-D samples was investigated by polarized optical microscopy. Optical micrographs of PLA stars (up to 6 arms) exist in the literature, where the encountered spherulites are generally described as “disordered” or “irregular”, which is imputed to the macroscopic defects caused by branching.[42,47,48] No information on the morphology of multi-arm PLA stars is currently available. Figure 3S presents the optical micrographs of the PAMAM-D samples isothermally crystallized at different temperatures – the range of crystallization of the sample PAMAM-D2 being obviously lower, in agreement with its lower melting point, as discussed above. “Normal”, quite well-developed, spherulitic superstructures with apparent Maltese cross patterns, having diameters going from tenths to hundredths of microns, were

observed in PAMAM-D1, whose texture got coarser on increasing the crystallization temperature, with more evident fibrosity and less clear (though still recognizable) Maltese crosses. Differently, PAMAM-D2 appeared more prone to crystallize dendritically: several small spherical open-textured polycrystalline aggregates were formed at low temperature, evolving into loose, branched dendrites (of increasing irregular shape) on increasing temperature. As it is known that, for crystallization from the melt, openness of texture and low frequency of branching (till dendritic growth), are related to the presence of an appreciable concentration of "impurities" which need to be rejected/segregated into the interfibrillar regions,[51,52] the morphological observation just confirms the existence of a large portion of non-crystallizable species (that is, molecules of lower molecular weight or more branched – with the requirements for crystallizability getting stricter the higher the temperature) in PAMAM-D2.

Characterization of PAMAM-D/L_{100K} Blend Films.

As the next step, the two synthesized dendritic star-like poly(D-lactide)s were introduced into commercial, high molecular weight, L_{100K} via solution casting: altogether, seven materials (that is, blends of L_{100K} with either 5, 25 or 50 wt% of PAMAM-D1, or 5 or 50 wt% of PAMAM-D2, plus neat L_{100K} and the 1:1 L_{100K}/D_{100K} blend) were fabricated as films and studied. DSC and WAXD techniques were exploited to investigate how the multi-arm star-like poly(D-lactide)s steer the structuring of PLA materials.

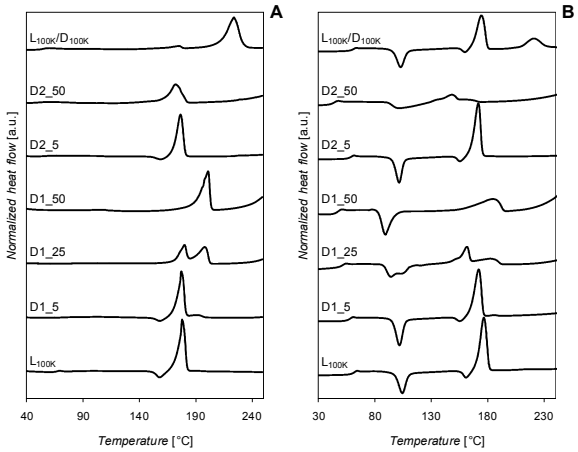

Fig. 3. DSC thermograms of the solution-cast films during the first heating scan (A), and during the second heating scan (*i.e.*, following cooling from the relaxed melt to -10 °C; B); the heat flow is normalized to the PLA content.

Figure 3 shows the DSC heating thermograms of the PAMAM-D/L_{100K} blends, during the first and second heating scan as well (that is, on heating the as-cast film and after cooling from the relaxed melt), together with those of the "reference" L_{100K} and L_{100K}/D_{100K} materials (bottom and upper curves, respectively); the corresponding thermal data are given in Table 2 for all samples. The as-cast materials were too highly crystalline for the Tg to be discernible in most cases, unlike the instance of melt-cooled samples where all glass transitions can be detected clearly. As the crystalline content after melt-cooling was similar (similarly low) for all the samples (about 10% for the two reference materials, between 1 and 10% for the PAMAM-D/L_{100K} blends – D2_50 and D1_50 being the two extremes, the other blends ranging in-between, with the exact values not easy to be quantified due to the broad and weak crystallization peaks), considerations on the variation of the Tg with the composition of the blends can be done. In particular, it can be seen that all the curves exhibit only one glass transition step, with the trend to shift towards lower temperatures (with comparison to L_{100K} and L_{100K}/D_{100K}) the higher the amount of the PAMAM-D sample contained in the blend (see Figure 3B and Table 2). This is in agreement with the formation of miscible systems, whose Tg decreases proportionally on adding the lower-Tg PAMAM-D components – the effect of the more mobile PAMAM-D2 being, as expected, more marked. The DSC scans of the films obtained by solution casting (Figure 3A) reveal that, as for the PAMAM-D1/L_{100K} blend series, once PAMAM-D1 is merged into L_{100K}, an additional melting peak appears at about 200 °C. Since this peak is above the Tm of the pure homo-crystalline L_{100K} (at about 178 °C), it must be related to the formation of stereocomplex crystallites. Accordingly, as the content of PAMAM-D1 in the blend increases, the area of this peak increases too (going along with the amount of stereocomplex which can be formed between L_{100K} and the PDLA star oligomers), and simultaneously the intensity of the homo-crystal peak gets lower. Eventually, for D1_50, containing equimolar quantities of the two enantiomeric polymers, only the higher-temperature endotherm can be observed, which indicates the exclusive presence of stereocomplex crystallites (about 40%) in the solution-cast film. This behavior is different from that of the (also equimolar) commercial L_{100K}/D_{100K} blend, which still shows a small trace (corresponding to about 5%) of homochiral crystallites together with the (major – 40%) stereocomplex ones. The Tm of the stereocomplex crystallites formed in the PAMAM-D1/PLLA blends is much lower than the value measured for the L_{100K}/D_{100K} reference (about 224 °C, see Table 2), which is explained by the low arm-length,[41] as well as branched nature of PAMAM-D1 (factor disturbing not only its own crystallizability, but also that of its blends with linear PLLA).[27,28] The trends observed for the as-cast PAMAM-D1/L_{100K} films were found also during the second heating run; here, besides the glass transition, all the melt-cooled samples display cold-crystallization in addition to the melting peaks of the homo- and/or stereocomplex crystallites (Figure 3B). The sample D1_5 has a unique cold-crystallization peak, slightly anticipated with comparison to that of L_{100K} (see Table 2), which can be due to the little decrease of the Tg or to the nucleating action of the stereocomplex crystallites possibly formed during cooling.[53,54] The blend D1_25 presents a bimodal cold-crystallization exotherm, where the lower-temperature peak is most likely due to stereocomplex formation and the second peak corresponds to homo-crystallization (requiring longer induction time than stereocomplexation).[55] Further increasing the PAMAM-D1

amount, the first peak is shifted to lower temperatures, and it becomes dominant in the sample D1_50.

Correspondingly, the fraction of stereocomplex crystallites, as evaluated by the extent of the higher-temperature melting peak, increases with the PAMAM-D1 content, till complete predominance in the case of the equimolar blend. The melting peak of the stereocomplex crystallites is broader, and the Tm lower, for the melt/glass-crystallized samples than in their initial state from solution casting: this is a general observation, implying that the stereocomplex form obtained from solution is more ordered.[46,47] Also the melting peak of the homo-crystals is moved at lower temperatures with respect to L_{100K}, which has already been reported for melt-crystallized PLLA/PDLA blends and imputed to the less perfect structure of the homo-crystallites formed near/on the stereocomplex crystallites.[54] The result of the formation of stereocomplex crystallites in the PAMAM-D1/L_{100K} blends (included D1_5) on their cooling from the melt and subsequent heating up, is particularly remarkable if compared with the total absence of crystallinity of the pure PAMAM-D1 sample under the same treatment (see Figure 2A). This evidence can be explained by the higher crystallizability of the stereocomplex, whose minimum lactate sequence length for crystallization to occur is lower than that required for the crystallization of homo-crystals.[41] These data are somehow different than those obtained for blends of high-molar-mass PLLA with 4- and 6-arm PDLA star oligomers, that were reported to show off the unique presence of stereocomplex crystallites during the second heating scan also in the case of highly non-equimolar systems.[27,28] However, it must be pointed out that in both cases, unlike ours, the neat PLLA employed was not able to crystallize neither on melt-cooling nor glass-heating. Figure 3B evidences a most striking difference between the two equimolar blends D1_50, containing stereocomplex crystallites as the only crystalline species, and L_{100K}/D_{100K}, in which the stereocomplex crystallites coexist with a consistent fraction of homo-crystallites. This difference is much stronger than in the case of the as-cast films (see Figure 3A) as the critical molecular weight below which only stereocomplex crystallites are formed is lower for melt-crystallization (~6 x 10^3 g/mol) than for solution-casting (~4 x 10^4 g/mol, <28 x 10^4 g/mol if the other component has a very high molecular weight).[55,56] Commercial L_{100K} and D_{100K} are above these values, such that homo-crystallization occurs in their blend, where homochiral crystallites must consist of both homo-crystalline PLLA and PDLA (in contrast with those formed in the non-equimolar PAMAM-D1/L_{100K} blends, made only by the L_{100K} excess). The molecular weight of PAMAM-D1 is also above the critical value for solution- and melt-crystallization; notwithstanding this, it is able to afford exclusive stereocomplexation when blended with L_{100K}. Biela et al. have reported enhanced stereocomplexation in blends of multi-arm (*i.e.*, 13 or more) enantiomeric PLA stars.[57] However, we believe that the most likely explanation for the behavior of the PAMAM-D1/L_{100K} blends is that PAMAM-D1 has a high total mass but its arms are short, and this may promote a better miscibility and more ready interactions between L- and D-stereosequences, similar as the case of stereoblock-PLAs.[58] The DSC traces of the sample D2_5 do not reveal any presence of stereocomplex crystallites, while, based on the lower Tm and melting enthalpy as compared to its neat form, the crystallization of L_{100K} seems to be disturbed by the small amount of PAMAM-D2 (see Table 2). The as-cast D2_50 film displays a single melting peak (Figure 3A), whose temperature (around 172 °C) is even lower than that of the L_{100K} homo-crystallites. In principle, this peak can correspond either to very thin/defective stereocomplex crystallites, or to the melting of L_{100K} homo-crystallites formed in presence of high amount of the PAMAM-D2 "diluent". On heating up after cooling from the melt (Figure 3B), the sample D2_50 features a broad cold crystallization exotherm and a rather weak bimodal/double melting endotherm. Whatever the formed species are, it is evident the higher difficulty in forming crystals when the blends contain the more short-armed and densely-branched PAMAM-D2, which just reflects what already observed for pure PAMAM-D2 (see Figure 2A).

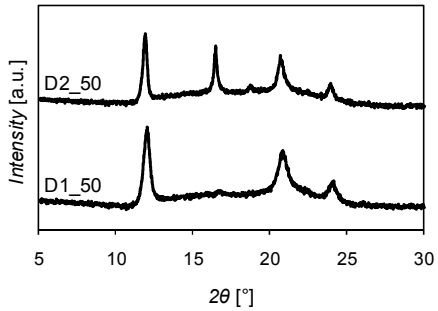

Fig. 4. WAXD profiles of the solution-cast PAMAM-D/PLLA blend films with equimolar content of PAMAM-D and PLLA.

WAXD was used to confirm/determine the crystalline structure of the solution-cast films. Figure 4 shows the diffractograms of the two equimolar PAMAM-D1/L_{100K} blends. The sample D1_50 exhibits the diffraction peaks characteristic of the stereocomplex crystallites at 2θ = 12, 21, and 24° alone,[29] thus corroborating the exclusive stereocomplex formation. From the deconvolution of the WAXD pattern, a crystalline content of about 45% was estimated, also in good agreement with the DSC data. Conversely, the crystal profile of the sample D2_50 contains additional peaks at 2θ = 17 and 19°, assigned to the α-form (or α'-form) of homo-crystals.[29,59] This reveals that both stereocomplex and homo-crystallites are present in the D2_50 blend, whose content was estimated to be around 30 and 10%, respectively. The possible explanations we suggest for this result are that, owing to its molecular features, not all the 50% fraction of PAMAM-D2 may be available for stereocomplex crystallization (this causing the presence of an excess of L_{100K} not involved in stereocomplexation), or, alternatively/simultaneously, that the stereocomplexation between L_{100K} and PAMAM-D2 may be too slow, such that at some point the homo-crystallization becomes competitive/dominant.

As expected, the morphological peculiarities already encountered in the multi-arm star-like poly(D-lactide)s are somehow mirrored in their equimolar blends with L_{100K} (see Figure 5, reporting as indicative the optical micrographs of the samples D1_50 and D2_50 isothermally crystallized at 155 °C and 130 °C, respectively). Indeed, in the whole explored temperature range (that is, 125-165 °C), D1_50 exhibits well-defined spherulites (which, as inferable on the basis of their melting temperature, are made of stereocomplex crystallites only), having a fairly compact texture – the only

indication for the presence of a small concentration of less crystallizable species, which are rejected radially, being the observation of jagged and flattened profiles at impending contacts between spherulites.[52] Conversely, Figure 5B shows that the sample D2_50 contains two types of spherulites (which evidence was observed in the whole explored range 120-145°C): the first-formed "internal" ones (assigned as stereocomplex spherulites involving PAMAM-D2 and, accordingly, characterized by an impurity-segregation-led fibrous sheaf-like structure),[51,52] and the larger, finer and brighter homocrystallites-made spherulites, nucleated in the melt or, mostly, cross-nucleated[60] on the stereocomplexed ones, which are thus "englobed".

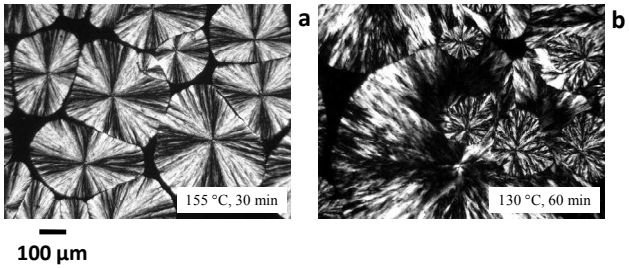

Fig. 5. Optical micrograph of the samples D1_50 (a) and D2_50 (b) isothermally crystallized from the melt at the indicated temperatures for the indicated times.

Co-existence of (darker) stereocomplex spherulites and (brighter) homocrystalline ones was previously reported by Tsuji et al. for highly asymmetric PLLA/PDLA blends,[55] as well as by Brochu et al. for asymmetric blends of enantiopure PLLA with a stereodefective PDLA where the formation of homochiral crystals is faster than that of the stereocomplexes, such that the crystallization of the homopolymer in excess is favored once that the spherulites of stereocomplex, acting as nucleation sites, are formed.[61] The evidences from optical microscopy thus support the above results and conclusions.

Upon introduction of PAMAM-D1 and PAMAM-D2 into L_{100K}, the resulting materials exhibit a higher thermal stability (see Figure 4S). This result could have been easily predicted in light of the well-known superior thermal stability of the stereocomplex – the peculiar strong interactions between PLLA and PDLA chains decreasing their mobility, thus retarding thermal degradation.[62] Moreover, the synergic effect of the global increase of the molecular weight of the system needs to be taken into account, whereby the concentration of the hydroxyl terminal groups (where cyclic oligomers and monomers are formed)[50] is much lowered with comparison to the starting star-like products.

Summarizing findings, the blends containing equimolar amounts of L_{100K} and our multi-arm star-like poly(D-lactide)s proved capable of full (or preponderant) stereocomplexation – both star oligomers having arms longer than the critical value for stereocomplex formation,[41] but the crystal fraction and characteristics being strongly dependent on the star structure – whereby these materials are expected to exhibit different (stereocomplex) properties while carrying the PAMAM units strongly anchored to the PLA matrix through the stereocomplex crystal regions.

Properties of PAMAM-D/L_{100K} Blend Films.

The incorporation of the hydrophilic PAMAM moieties into the hydrophobic PLA matrix is expected to enhance the hydrophilicity of the resulting materials, which should be reflected in their capability to absorb water. Indeed, while both the L_{100K} and L_{100K}/D_{100K} films do not show any tendency to uptake water, the blends D1_50 and D2_50 display a significant intrinsic absorbency (18% for the sample D1_50 and 21% – at least – for the PAMAM-richer D2_50; see Table 1S). From the values reported in Table 1S, it can be seen how the percentage of water absorbed correlates not only with the content of the PAMAM units in the material, as just evidenced, but also with their exposure on the surface of the films (as exemplified by the sample D1_25, whose water absorption, notwithstanding the non-negligible amount of PAMAM, is equal to zero, which we did explain as if the PAMAM sites were mainly embedded inside the film and not enough of them were easily accessible from outside for the water molecules to interact). Moreover, a weight loss was registered for the D2_50 specimens when immersed in water for the duration of the test (see Table 1S), to be imputed to the migration of water-soluble products – likely the (lower-molecular-weight, PAMAM-richer) fraction not involved in the crystalline regions – into the water phase. This observation points out not only the extreme importance of having the water-soluble PAMAM functionalities anchored to the PLA matrix, but also the impact that the constitutional features of the star-like poly(D-lactide)s can have on the actual performances of the obtained stereocomplexed PLA materials.

PAMAM dendrimers are well-known for their capability to bind metal ions to their interior, which results from their unique functional architecture:[4,5] if the PAMAM units are effectively available on the surface of the films, the blended materials are likely to maintain this capacity. To verify it, the samples L_{100K}, D1_50 and D2_50 were tested for Pd(II) uptake as described in the experimental section: after 48 hours contact at room temperature with the (orange-colored) Pd(II) acetate solution (and subsequent washings), a significant change of color to orange could be discerned for the D1_50 and D2_50 specimens – containing about 5.5 and 8 wt% of PAMAM, respectively – while the neat L_{100K} film was almost unchanged (Figure 6)

Fig. 6. Photographs of the samples L_{100K} (A) and D1_50 (B) after 48 hours of immersion at room temperature in the Pd(II) acetate solution, and D1_50 (C) immersed for 1 hour at 80 °C (all the samples were washed before the pictures).

This (qualitative) observation was supported by the ICP-OES analysis, according to which the quantity of Pd(II) retained by the samples L_{100K}, D1_50 and D2_50 was 0.04, 0.6 and 0.5 wt%,

respectively. The sample L_{100K}/D_{100K}, subjected to the same treatment, was measured to retain a quantity of Pd(II) of 0.03 wt%. These data clearly show that the polymer matrix has no ability to bind Pd ions (nor the presence of the stereocomplex crystals produces it – as we had already demonstrated in the case of electrospun stereocomplex fibers),[63] and it is the PAMAM moieties to allow such interaction (namely complexation) by virtue of the amino functional groups in their framework,[6,7] so that a relevant amount of Pd(II) (that is, more than ten times higher than for the reference L_{100K}) can be sorbed. The reason why the Pd(II) uptake seems not proportional to the PAMAM content in the film is that a 20% of matter was lost during the immersion in acetonitrile for the sample D2_50 (whereas weight losses were negligible in the case of the other samples), likely caused, again, by the leaching of the shorter-armed (crystal-unbound) PAMAM-D2 molecule fraction. After 1 hour dip in the Pd(II) acetate solution at 80 °C (and subsequent washings), the sample D1_50 turned black (which is indicative of the presence of reduced Pd; see Figure 6), and the ICP_OES measurement revealed a 2.0 wt% of linked metal: the enhancement of the Pd-uptake-ability caused by temperature is evident, such that we calculated that in these conditions a 10 × 10 cm^2 sized film would be sufficient to remove all the 10 mg of Pd(II) from a homogeneous reaction medium. It needs to be emphasized that both the L_{100K} and the D2_50 specimens were found to be completely dissolved in acetonitrile at 80 °C, this pointing out the benefits of having stereocomplexed materials, provided that their properties are properly optimized.

Conclusions

In this work, we developed a PLA-based system capable of supporting dendritic/star-like molecules, combining the properties of the stereocomplex PLA matrix with those of PAMAM dendrimers. Indeed, our materials offer many advantages related to the employment of dendrimers, not only their immobilization onto an insoluble solid support, but also the easy processability of this support as a polymer, with some resistential characteristics, and having a "bio" nature.

In detail, two different poly(D-lactide)s were obtained via ROP of D-lactide using a generation 2 hydroxyl-terminated PAMAM dendrimer as macroinitiator, and subsequent fractionation in methanol. As determined by ^{1}H NMR and TGA analyses, this enabled the preparation of two star-like oligomers with molecular weights of about 30.000 and 20.000 g/mol, incorporating about 11 and 16% of PAMAM as the core, and differing for the length (about 2500 and 1000 g/mol, respectively) and number (about 11-12 and 14-15, respectively) of the attached PDLA arms. As the next stage, the two synthesized dendritic star-like poly(D-lactide)s were introduced into a commercial, high molecular weight, linear PLLA via solution casting, to produce either equimolar or non-equimolar blend films. The multi-arm PDLA stars were found to be easily involved in the formation of stereocomplexes during both solution and melt crystallization, till exclusive/preponderant stereocomplexation in the equimolar blends, so that the PAMAM units are anchored to the PLA matrix, and with the stereocomplex content and characteristics strongly depending on the star structure. Unlike the neat PLA matrix, and thanks to the incorporation of the PAMAM functionalities, the equimolar blends proved to possess significant water-absorbency (up to about 20%), and Pd(II)-uptake-ability – this latter increasing on increasing temperature (up to 2.0 wt%) – such that we could show the employment of one of our material film to remove Pd catalyst from an homogeneous reaction medium as a typical organic reaction system. Release of matter from the films was observed in either water or acetonitrile at room temperature when it was the lower-molecular-weight, more short-armed and densely-branched PDLA oligomer to be blended with PLLA, as not all of its 50% fraction could be involved in the formation of the stereocomplex, whose thermal resistance also turned out to be insufficient for the high-temperature-Pd(II)-uptake-application. We believe the potential of these materials to be huge when combining the thermal and chemical resistance of the stereocomplex with the properties afforded by the PAMAM units – with the PAMAM dendrimers recognized as suitable for a number of applications, such as scaffold for zerometal clusters (think for example about the electrospinning of these materials to prepare nanofibers decorated with metal nanoclusters, to be used as catalyst)[63,64] or binding of drugs/biological substates.[2,3] Moreover, our systems are fully biocompatible, making them attractive for biomedical applications, with the material properties and degradation being easily tunable by adjusting the stereocomplex content and characteristics (that is, through the structure of the star-like oligomers).

Acknowledgements

We are grateful to PURAC BIOCHEM (The Netherlands) for supplying the lactide monomers and to the Italian Ministry of Education and University through the 2010-2011 PRIN project (Grant No. 2010XLLNM3_005). The authors thank F. Drago and S. Nitti for support in the ICP characterization.

References

1 D.A. Tomalia, H. Baker, J. Dewald, M. Hall, G. Kallos, S. Martin, J. Roeck, J. Ryder and P. Smith, *Polym. J.*, 1985, **17**, 117.
2 K. Inoue, *Prog. Polym., Sci.* 2000, **25**, 453.
3 U. Gupta, H.B. Agashe, A. Asthana and N.K. Jain, *Biomacromolecules*, 2006, **7**, 649.
4 D. Astruc, E. Boisselier and C. Ornelas, *Chem. Rev.*, 2010, **110**, 1857.
5 V. Sue Myers, M.G. Weir, E.V. Carino, D.F. Yancey, S. Pande and R.M. Crooks, *Chem. Sci.*, 2011, **2**, 1632.
6 M. Zhao and R.M. Crooks, *Angew. Chem. Int. Ed.*, 1999, **38**, 364.
7 D. Tabuani, O. Monticelli, H. Komber and S. Russo, *Macromol. Chem. Phys.*, 2003, **204**, 1576.
8 E. De Jesús and J.C. Flores, *Ind. Eng. Chem. Res.*, 2008, **47**, 7968.
9 J.P. Reynhardt and H. Alper, *J. Org. Chem.*, 2003, **68**, 8353.
10 Y. Jiang and Q. Gao, *J. Am. Chem. Soc.*, 2006, **128**, 716.
11 A.V. Biradar, A.A. Biradar and T. Asefa, *Langmuir*, 2011, **27**, 14408.
12 Q. Zhang, N. Wang, L. Zhao, T. Xu and Y. Cheng, *ACS Appl. Mater. Interfaces*, 2013, **5**, 1907.
13 Y. Niu, R. Qu, H. Chen, L. Mu, X. Liu, T. Wang, Y. Zhang and C. Sun, *J. Hazard. Mater.*, 2014, **278**, 267.

14 X.Z. Wu, P. Liu, Q.S. Pu, Q.Y. Sun and Z.X. Su, *Talanta*, 2004, **62**, 918.
15 Y.-L. Zhao, Q. Cai, J. Jiang, X.-T. Shuai, J.-Z. Bei, C.-F. Chen and F. Xi, *Polymer*, 2002, **43**, 5819–5825.
16 Y.-L. Zhao, X.-T. Shuai, C.-F. Chen and F. Xi, *Chem. Mater.*, 2003, **15**, 2836.
17 Q. Cai, Y. Zhao, J. Bei, F. Xi and S. Wang, *Biomacromolecules*, 2003, **4**, 828.
18 F. Wang, T.K. Bronich, A.V. Kabanov, D. Rauh and J. Roovers, *Bioconjugate Chem.*, 2008, **19**, 1423.
19 D.J.A. Cameron and M.P. Shaver, *Chem. Soc. Rev.*, 2011, **40**, 1761.
20 M. Adeli and R. Haag, *J. Polym. Sci., Part A: Polym. Chem.*, 2006, **44**, 5740.
21 C.-X. Zhang, B. Wang, Y. Chen, F. Cheng and S.-C. Jiang, *Polymer*, 2012, **53**, 3900.
22 T. Ouchi, T. Kontani and Y. Ohya, *Polymer,* 2003, **44**, 3927.
23 T. Ouchi, S. Ichimura and Y. Ohya, *Polymer,* 2006, **47**, 429.
24 Y. Phuphuak, Y. Miao, P. Zinck and S. Chirachanchai, *Polymer*, 2013, **54**, 7058.
25 Y. Phuphuak and S. Chirachanchai, *Polymer*, 2013, **54**, 572.
26 J. Geschwind, S. Rathi, C. Tonhauser, M. Schömer, S.L. Hsu, E.B. Coughlin and H. Frey, *Macromol. Chem. Phys.,* 2013, **214**, 1434.
27 S. Inkinen, M. Stolt and A. Södergård, *Polym. Adv. Technol.*, 2011, **22**, 1658.
28 S.R. Andersson, M. Hakkarainen, S. Inkinen, A. Södergård and A.-C. Albertsson, *Biomacromolecules*, 2012, **13**, 1212.
29 H. Tsuji, *Macromol. Biosci.*, 2005, **5**, 569.
30 Y. Sun, and C. He, *RSC Adv.,* 2013, **3**, 2219.
31 M. Brzeziński, M. Bogusławska, M. Ilčíková, J. Mosnáček, and T. Biela, *Macromolecules,* 2012, **45**, 8714.
32 M. Brzeziński and T. Biela, *Materials Letters,* 2014, **121**, 244.
33 Y. Sun, and C. He, *ACS Macro Lett.,* 2012, **1**, 709.
34 Y. Sun, and C. He, *Macromolecules*, 2013, **46**, 9625.
35 D. Garlotta, *J. Polym. Environ.*, 2002, **9**, 63–83.
36 ASTM D570-98(2010)e1,"Standard Test Method for Water Absorption of Plastics", ASTM International, West Conshohocken, PA, 2010, www.astm.org.
37 P. Degée, P. Dubois, S. Jacobsen, H.G. Fritz and R. Jérôme, *J. Polym. Sci., Part A: Polym. Chem.*, 1999, **37**, 2413–2420.
38 Y. Huang, U.S. Patent 2005/0238618 A1, 2005.
39 H. Korhonen, A. Helminen and J.V. Seppälä, *Polymer,* 2001, **42**, 7541.
40 B.H. Stuart, *Infrared Spectroscopy: Fundamemntals and Applications*, John Wiley & Sons Ltd: Chichester, 2004.
41 S.J. de Jong, W.N.E. van Dijk-Wolthuis, J.J. Kettenes-van den Bosch, W.E. Schuyl and P.J.W. Hennink, *Macromolecules*, 1998, **31**, 6397.
42 Q. Hao, F. Li, Q. Li, Y. Li, L. Jia, J. Yang, Q. Fang and A. Cao, *Biomacromolecules*, 2005, **6**, 2236.
43 B. Atthoff, M. Trollsås, H. Claesson and J.L. Hedrick, *Macromol. Chem. Phys.*, 1999, **200**, 1333.
44 E.S. Kim, B.C. Kim and S.H. Kim, *J. Polym. Sci., Part B: Polym. Phys.*, 2004, **42**, 939.
45 W. Zhang and S. Zheng, *Polym. Bull.*, 2007, **58**, 767.
46 S. Saeidlou, M.A. Huneault, H. Li and C.B. Park, *Prog. Polym. Sci.*, 2012, **37**, 1657.
47 H. Tsuji, T. Miyase, Y. Tezuka and S.K. Saha, *Biomacromolecules*, 2005, **6**, 244.
48 L. Wang and C.-M. Dong, *Polym. Sci., Part A: Polym. Chem.*, 2006, **44**, 2226.
49 C. Gottschalk, F. Wolf and H. Frey, *Macromol. Chem. Phys.*, 2007, **208**, 1657.
50 K. Jamshidi, S.-H. Hyon and Y. Ikada, *Polymer,* 1988, **29**, 2229.
51 P.H. Geil *Polymer single crystals*, Interscience: New York, 1963.
52 H.J Keith and Jr. F.J. Padden, *J. Appl. Phys.*, 1964, **35**, 1270.
53 S.C. Schmidt and M.A. Hillmyer, *J. Polym. Sci., Part B: Polym. Phys.*, 2001, **39**, 300.
54 H. Yamane and K. Sasai, *Polymer*, 2003, **44**, 2569.
55 H. Tsuji and Y. Ikada, *Macromolecules*, 1993, **26**, 6918.
56 H. Tsuji, S.-H. Hyon and Y. Ikada, *Macromolecules*, 1991, **24**, 5651.
57 T. Biela, A. Duda and S. Penczek, *Macromolecules*, 2006, **39**, 3710.
58 M. Kakuta, M. Hirata and Y. Kimura, *J. Macromol. Sci., Polym. Rev.*, 2009, **49**, 107.
59 P. Pan, B. Zhu, W. Kai, T. Dong and Y. Inoue, *J. Appl. Polym. Sci.*, 2008, **107**, 54.
60 D. Cavallo, L. Gardella, G. Portale, A.J. Müller and G.C. Alfonso, *Polymer*, 2013, **54**, 2528.
61 S. Brochu, R.E. Prud'homme, I. Barakat and R. Jérôme, *Macromolecules*, 1995, **28**, 5230.
62 H. Tsuji and I. Fukui, *Polymer*, 2003, **44**, 2891.
63 O. Monticelli, M. Putti, L. Gardella, D. Cavallo, A. Basso, M. Prato and S. Nitti, *Macromolecules*, 2014, **47**, 4718.
64 L. Gardella, A. Basso, M. Prato and O. Monticelli, *ACS Appl. Mater. Inter.*, 2013, **5**, 7688.

For Table of Contents Graphical Abstract Use Only

On stereocomplexed polylactide materials as support for PAMAM dendrimers: synthesis and properties

Lorenza Gardella, Andrea Basso, Mirko Prato, Orietta Monticelli

Synthesis of a PLA-based system capable of supporting dendritic/star-like molecules, combining the properties of the stereocomplex PLA matrix with those of PAMAM dendrimers